

Support effects in Pt/TiO₂–ZrO₂ catalysts for NO reduction with CH₄

R. Mariscal^a, S. Rojas^a, A. Gómez-Cortés^b, G. Díaz^b, R. Pérez^c, J.L.G. Fierro^{a,*}

^a Instituto de Catálisis y Petroleoquímica, CSIC, Cantoblanco, 28049 Madrid, Spain

^b Department of Physical Chemistry, Institute of Physics UNAM, P.O. Box 20-364, Mexico 01000, Mexico

^c UAEM, Faculty of Chemistry, Mexico

Abstract

ZrO₂–TiO₂ mixed oxides, prepared using the sol–gel method, were used as supports for platinum catalysts. The effects of catalyst pre-reduction and surface acidity on the performance of Pt/ZT catalysts for the reduction of NO with CH₄ were studied. The diffuse reflectance infrared Fourier transformed (DRIFT) spectra of CO adsorbed on the Pt/ZT catalysts, and also on the Pt/T and Pt/Z references, pre-reduced at 773 K in hydrogen, revealed that an SMSI state is developed in the Ti-rich oxide-supported platinum catalysts. However, no shift in the binding energy of Pt 4f_{7/2} level for Pt/T and Pt deposited on Ti-rich support counterparts pre-reduced at 773 K was found by photoelectron spectroscopy. The DRIFT spectra of the catalysts under the NO+O₂ co-adsorption revealed the appearance of nitrite/nitrate species on the surface of the Zr-containing catalysts, which displayed acidic properties, but were almost absent in the Pt/T catalyst. The intensity of these bands reached a maximum for the Pt/ZT(1:1) catalyst, which in turn exhibited a larger specific area. In the absence of oxygen in the feed stream, the NO + CH₄ reaction showed DRIFT spectra assigned to surface isocyno species. Since the intensity of this band is higher for the Pt/ZT (9:1) catalyst, it seems that such species are developed at the Pt–support interface. © 2002 Elsevier Science B.V. All rights reserved.

Keywords: Emission control; Nitrogen oxides; Selective catalytic reduction; Methane; Pt/ZrO₂–TiO₂ catalysts

1. Introduction

The stringent regulations imposed by the EU to control exhaust emissions from car engines have led to the development of catalytic systems able to perform the simultaneous removal of gaseous contaminants. Selective catalytic reduction (SCR) by hydrocarbons, and specifically by CH₄, seems to be the technology of choice. The attempt to use methane as a reduction agent has been additionally hampered by its relative inertness, which provides lower activity than other reduction gases over most catalytic systems [1,2]. Thus,

in recent years much effort has focused on developing good SCR catalysts that will be active, selective and stable for long periods of time, using methane as a reduction agent [3,4].

Although platinum is considered the best metal candidate for the SCR reaction, doubts exist concerning the type of support to be used. It has been shown that TiO₂–ZrO₂ systems can be satisfactorily used for this reaction because the mixed oxide displays unusual acid properties and very high thermal resistance with respect to its individual ZrO₂ and TiO₂ components [5]. The latter property appears of paramount importance because the activation of the C–H bond of CH₄ occurs at rather high temperatures. Moreover, it has been reported recently [6] that the addition of ZrO₂ to TiO₂ may prevent the migration of TiO₂ onto the metal

* Corresponding author. Tel.: +34-91-585-4769;
fax: +34-91-585-4760.
E-mail address: jlgfierro@icp.csic.es (J.L.G. Fierro).

surface, after reduction at high temperature. Thus, the possible ‘strong metal-support interaction’ (SMSI), which is known to be developed upon reduction of the catalysts at high temperature can be inhibited.

It has been recognised that the most active catalysts are associated with strongly acidic zeolites [7–9] and non-zeolitic acidic supports, such as $\text{SO}_4^{2-}/\text{ZrO}_2$ or binary oxides [10]. Thus, our aim in the present work was to investigate the surface characteristics of TiO_2 – ZrO_2 -supported platinum catalysts and to explain the enhancement in the turnover frequency (TOF) of the SCR reaction been observed in these catalysts prepared with TiO_2 – ZrO_2 supports on the Zr-rich composition side (Zr:Ti = 9 molar ratio).

2. Experimental

The single TiO_2 and ZrO_2 oxides and the binary ZrO_2 – TiO_2 (9:1, 1:1 and 1:9 molar ratios) were prepared using the sol–gel method. Basically, the Ti- and Zr-alkoxide precursors were hydrolysed with an NH_4OH –ethanol solution. The xerogel samples were calcined at 773 K for 5 h. The supports prepared were impregnated with the H_2PtCl_6 solution at an appropriate concentration to yield a 1 wt.% Pt. The catalysts obtained were calcined at 773 K for 2 h and activated by reduction with hydrogen at 773 K for 1 h.

Specific surface areas were calculated by the BET method from the nitrogen adsorption isotherms, determined by the single-point method using a 30% N_2/He gas mixture, recorded at the temperature of liquid nitrogen. X-ray diffraction (XRD) powder patterns were recorded with a Siemens D-500 diffractometer, using nickel-filtered $\text{Cu K}\alpha$ ($\lambda = 0.15406 \text{ nm}$) radiation. All samples were scanned in the range between $2\theta = 15^\circ$ and 70° . Diffractograms were recorded at a step width of 0.025° and by counting 12 s at each step.

Diffuse reflectance infrared Fourier transformed (DRIFT) spectra were collected on a Nicolet-510 FTIR spectrophotometer working at a resolution of 4 cm^{-1} , using a Harrick HVC-DRP environmentally controlled cell. About 30 mg of the powdered sample was packed in a sample holder and pretreated in situ in the DRIFT cell under a H_2 flow. Temperature was increased at a rate of 10 K/min up to 773 K and then kept for 1 h. The sample was subsequently cooled to room temperature prior to exposure to the reactant

mixture. The spectrum of dry KBr was taken for IR single-beam background subtraction. The IR spectra were collected at each temperature by increasing the cell temperature and holding at the desired temperature while collecting 256 scans.

Photoelectron spectra were acquired with a VG Escalab 200R spectrometer equipped with a hemispherical electron analyser and an $\text{Mg K}\alpha$ (1253.6 eV, $1 \text{ eV} = 1.6022 \times 10^{-19} \text{ J}$) X-ray exciting source. Samples were mounted on a sample rod placed in the pretreatment chamber and evacuated at 353 K for 1 h prior to being moved to the analysis chamber. During data acquisition, the pressure in the ion-pumped analysis chamber was below $3 \times 10^{-9} \text{ mbar}$. O 1s, Ti 2p, Zr 3d and Pt 4f core-level spectra were recorded. Intensities were estimated by calculating the integral of each peak after subtraction of the ‘‘S-shaped’’ background and fitting the experimental curve to a combination of Lorentzian and Gaussian lines of variable proportions [11]. The C 1s peak at a binding energy of 284.9 eV was taken as internal standard. Using this reference, binding energies were determined with an accuracy of $\pm 0.1 \text{ eV}$.

3. Results and discussion

The labelling and specific area values of different catalysts are shown in Table 1. It may be observed that specific area for platinum supported on pure ZrO_2 and TiO_2 oxides was moderate (ca. $50 \text{ m}^2/\text{g}$) but substantially lower than for the ZT (9:1) and ZT (1:9) compositions (ca. $180 \text{ m}^2/\text{g}$). For the intermediate composition ZT (1:1), BET area was exceptionally high, proving to be almost 10-fold higher than for the single oxides.

XRD patterns were recorded for all calcined catalysts. The XRD pattern of the Pt/Z sample exhibited

Table 1
Labelling and specific BET area of Pt/ ZrO_2 – TiO_2 catalysts

Catalysts (molar ratio) ($\text{ZrO}_2/\text{ZrO}_2 + \text{TiO}_2$)	Labelling	Specific area (m^2/g)
Pt/ ZrO_2	Pt/Z	42
Pt/ ZrO_2 – TiO_2 (0.9)	Pt/ZT (9:1)	181
Pt/ ZrO_2 – TiO_2 (0.5)	Pt/ZT (1:1)	465
Pt/ ZrO_2 – TiO_2 (0.1)	Pt/ZT (1:9)	177
Pt/ TiO_2	Pt/T	50

diffraction lines of tetragonal and monoclinic phases of ZrO_2 , the former phase being dominant. For the Pt/T sample, only the TiO_2 anatase phase was detected. Pt/ZT (9:1), with a Zr-rich composition, showed only the diffraction lines of the tetragonal ZrO_2 phase, whereas the Pt/ZT (1:9) counterpart, with a Ti-rich composition, exhibited the diffraction lines of the anatase TiO_2 phase. By contrast, no diffraction lines of either ZrO_2 or TiO_2 crystalline phases were observed in the XRD pattern of the Pt/ZT (1:1) catalyst, which is consistent with an amorphous material. No evidence of Pt phase was observed by XRD in either the pure or mixed oxide supports, indicating that platinum phases are highly dispersed on the surface of the individual (Z and T) or mixed (ZT) oxides.

3.1. Influence of pretreatments on exposed platinum

TOF values for the reduction of NO with CH_4 were determined for all the catalysts over a wide range of reaction temperatures. It was observed that at intermediate temperatures TOF was substantially higher for the Pt/ZTi (9:1) catalyst [12] than for the other members of the ZT series and for the single Pt/Z and Pt/T catalysts. To understand this type of behaviour, the nature of exposed Pt atoms on the catalyst surface was revealed by recording the DRIFT spectra of the adsorbed CO probe. Study of irreversible CO adsorption basically included: (i) passing a flow of 5% CO/He gas mixture over the Pt/ TiO_2 – ZrO_2 catalyst at 298 K for 15 min; (ii) purging under a flow of He (50 ml/min) for 15 min to remove gas phase and reversibly adsorbed species; (iii) heating from 298 to 773 K.

Infrared spectra of the CO adsorbed on the Pt-supported catalysts are shown in Fig. 1A. For the Zr-rich composition, the catalyst (Pt/ZT (9:1)) showed a broad band, with a maximum at 2065 cm^{-1} , plus two additional shoulders at high (ca. 2080 cm^{-1}) and low (ca. 2020 cm^{-1}) frequency. The dominant maximum may be assigned to the CO probe linearly bonded to metallic platinum atoms located on high-index crystal faces, the high and low frequency shoulders resulting from adsorption at metallic sites with high or low unsaturated co-ordination, respectively [13–15]. On the other hand, the intensity of the band of CO adsorbed at ambient temperature onto the Ti-rich supported

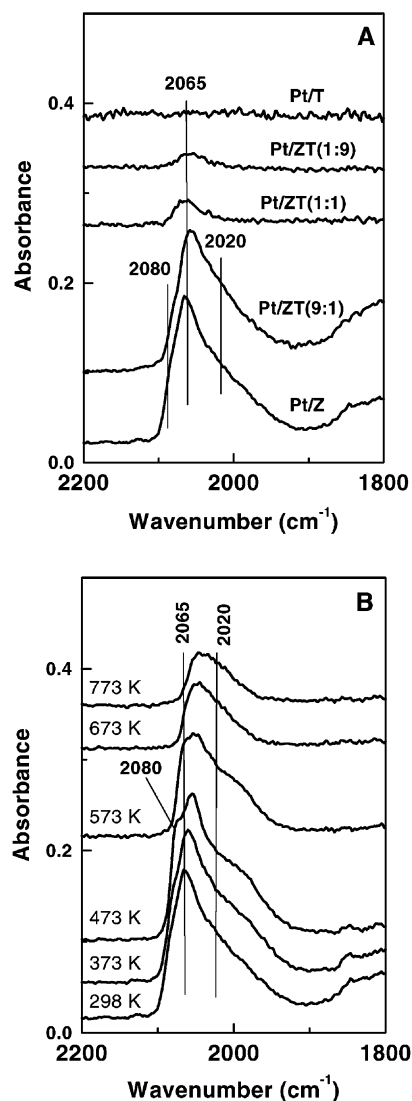


Fig. 1. (A) DRIFT spectra of CO adsorption on Pt/ZT catalysts reduced at 773 K for 1 h. (B) Evolution of CO infrared bands on Pt/Z catalyst with pre-adsorbed CO and then purged in a helium flow at temperatures in the 298–773 K range.

catalyst was very low; it decreased from Pt/ZT (1:1) to Pt/ZT (1:9) sample and vanished for Pt/T. It is evident that CO chemisorption on Pt crystallites deposited on TiO_2 particles or micro-domains becomes inhibited upon catalyst reduction [13]. This finding suggests that an SMSI state would be developed on the metallic function of the catalyst.

Table 2

Binding energy (eV) of core-electrons and surface atomic ratios of catalysts subjected to different pretreatments

Catalyst	Ti 2p _{3/2}	Zr 3d _{5/2}	Pt 4f _{7/2}	Pt/Ti (Pt/Zr)	Zr/Ti atom
Pt/T (vacuum)	458.5	–	74.0	0.0067	–
Pt/T, H ₂ (473 K)	458.5	–	70.7	0.0098	–
Pt/T, H ₂ (773 K)	458.5	–	70.4	0.0100	–
Pt/ZT (1:9), H ₂ (773 K)	458.5	182.2	70.6	0.0101	0.087
Pt/ZT (1:1), H ₂ (773 K)	458.7	182.2	71.0	0.0104	1.47
Pt/ZT (9:1) (vacuum)	458.7	182.0	72.5	0.0081	13.1
Pt/ZT(9:1), H ₂ (473 K)	458.8	182.1	72.4	0.0089	13.1
Pt/ZT(9:1), H ₂ (773 K)	458.7	182.0	71.4	0.0087	12.1
Pt/Z (vacuum)	–	182.2	72.8	0.0085	–
Pt/Z, H ₂ (473 K)	–	182.2	72.8	0.0086	–
Pt/Z, H ₂ (773 K)	–	182.2	71.4	0.0095	–

In order to gain insight into the thermal stability and temperature-dependent frequency shift for linear carbonyl bands, the Pt/Z catalyst was selected. The DRIFT spectra of CO pre-adsorbed on the Pt/Z catalyst followed by heating at temperatures from 298 to 773 K are shown in Fig. 1B. Upon heating, the DRIFT bands progressively shifted to lower frequencies and band intensity decreased, as expected, although the bands were still observable at temperatures as high as 773 K. The shift to lower frequency would indicate a reduction in dipole–dipole interactions as the number of neighbouring CO molecules diminishes with decreasing surface coverage.

Photoelectron spectra of all the samples in both the calcined state and after pre-reduction in hydrogen at 473 and 773 K were recorded. The binding energy of Zr 3d_{5/2}, Ti 2p_{3/2} and Pt 4f_{7/2} core-levels of such samples and pretreatments are shown in Table 2. In addition, the Pt 4f_{7/2} spectra of the reference Pt/Z sample are shown in Fig. 2. On scrutinising the binding energy of the Pt 4f_{7/2} peak, it is clear that there are substantial differences, depending on the carrier used and pretreatments. In the calcined samples, platinum was oxidised to Pt²⁺, but it became reduced when exposed to hydrogen at 473 K. For the Pt/Z and Pt deposited on Zr-rich supports, reduction is more difficult but it is complete at 773 K. A significant difference in the catalysts pre-reduced at 773 K is that the binding energy of the Pt 4f_{7/2} peak is lower for Pt/T, typical of Pt⁰, increases slowly with increasing Zr-content, and reaches the highest value (ca. 1 eV) for the Pt/Z counterpart. In accordance with the DRIFT data shown in Fig. 1, a metallic state exists in all the catalysts;

however, the higher binding energies of the Pt 4f_{7/2} peak in Zr-containing samples might be due to the interaction of the Pt clusters with the acid sites of the zirconia phase, but in no case resulting from an SMSI state.

Quantitative XPS data, also depicted in Table 2, indicate that platinum dispersion levels are only slightly higher in the Ti-rich supports. Since the Pt 4f signal is

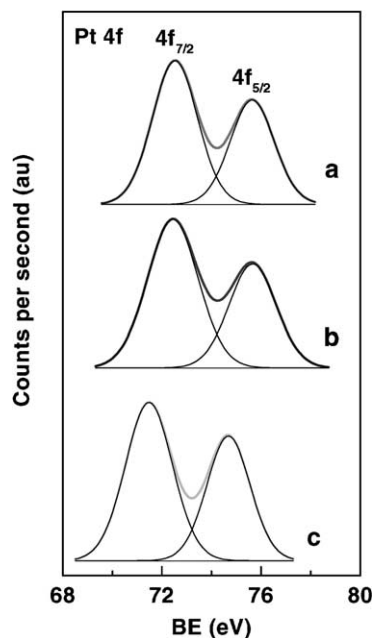


Fig. 2. Pt 4f core-level spectra of Pt/Z catalyst subjected to various pretreatments: (a) vacuum; (b) reduction in H₂ at 473 K for 1 h; (c) reduction in H₂ at 773 K for 1 h.

not depleted upon pre-reduction at 773 K, in principle the migration of TiO_x fragments onto the Pt particles may be ruled out. From these data, it can be inferred that, presumably, electronic effects, which do not affect core-levels to a significant extent but do strongly modify the chemisorption properties of the metal particles, are involved. Quantification of the Zr/Ti surface ratios was also possible. Zirconia segregation takes place in ZT (1:1) and ZT (9:1) supports. However, the opposite trend is observed in the ZT (1:9) support.

3.2. Influence of acidity on NO oxidation

For the mechanism of the SCR reaction of NO_x with CH_4 in the presence of excess oxygen, it is widely accepted that the key step of the reaction is the transformation of NO into NO_2 [16–18]. Several authors have reported that the role of acid sites is to promote the NO oxidation step [7–10,19]. Most such studies were mainly devoted to zeolite-based catalysts although a few of them have concentrated on some metal oxides. Therefore, acid sites are responsible, in part, for the oxidation of NO, which in turn is a key step in the selective catalytic reaction of NO with CH_4 in excess oxygen. Moreover, it is well known that ZrO_2 – TiO_2 mixed oxides exhibit high surface acidity as a consequence of the charge imbalance resulting from the generation of Zr–O–Ti bonds, and that the acid sites on ZrO_2 – TiO_2 mixed oxides play an important role for this reaction.

DRIFT spectra of Pt/Z, Pt/T and Pt/ZT catalysts exposed to an $\text{NO} + \text{O}_2$ gas mixture were recorded with the aim of evaluating the influence of surface acidity on the nature and amount of different surface species. All the catalysts were pre-reduced in a flow of H_2 at 773 K, cooled to 298 K, and subsequently exposed to a flow of NO (3000 ppm in Ar) and 5% O_2 gas mixture. The DRIFT spectra were recorded after 15 min of passing the flow of the $\text{NO} + \text{O}_2$ mixture over the catalyst. Fig. 3 shows infrared spectra in the 1800–1100 cm^{-1} range for all the samples. All the peaks observed may be assigned to nitrite/nitrate species [18,20]. In general, peak positions are similar for all the catalysts, although peak intensity is quite different. For the Pt/Z catalyst, the intensity of the nitrates bands is smaller than for the Pt/ZT catalysts oxides, but still much higher than for the Pt/T counterpart. This clearly indicates that the oxidation of NO by O_2 is irrelevant for the Pt/T catalyst, in

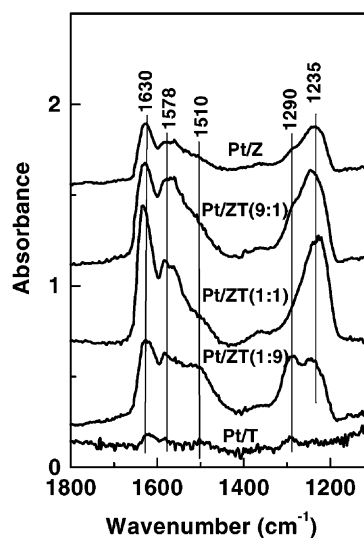


Fig. 3. DRIFT spectra of NO and O_2 co-adsorption at room temperature on Pt/ZT catalysts.

which TiO_2 surface acidity is extremely low, and substantially higher for the Pt/Z catalyst, which exhibits higher acidity. Among the binary oxides, the Pt/ZT (1:1) catalyst shows the highest intensity and also, as noted above, the largest BET area. From the spectra in Fig. 3 it is clear that all the Zr-containing catalysts, and particularly the binary ZT (9:1), ZT (1:1) and ZT (1:9) compositions, exhibit a higher acidity than the individual ZrO_2 and TiO_2 oxides. Thus, the oxidation of NO by O_2 and subsequent formation of surface nitrate species is intimately related to support acidity, which in turn depends on the specific area of the support and of the metal function (Pt). Moreover, taking into account that in the Ti-rich catalysts pre-reduced at 773 K few Pt atoms are exposed on the support surface, the reaction of NO and O_2 to yield NO_3^- mainly occurs at the interface of Pt particles with the acid sites of the carrier. In sum, NO_x^- ($x = 2, 3$) species are formed on the Lewis acid sites [13], and the proportion of these species on the catalyst surface runs in parallel with the specific area or Zr/Ti ratio.

3.3. Intermediate species in the $\text{NO} + \text{CH}_4$ reaction

The above experiments revealed the involvement of the SMSI state in the Ti-rich Pt/ZT catalysts along hydrogen pre-treatment at temperatures of 473 and

773 K. A second effect observed was the influence of surface acidity on the oxidation reaction of NO, which is a key step in the reaction of NO with CH₄ in the presence of an oxygen excess. Therefore, the acidity of the carrier, which is presumably dependent on the Ti/Zr ratio, might bring to bear some influence on the catalytic function of the platinum phase. This aspect is analysed below.

The DRIFT spectra of the Pt/Z, Pt/ZT (9:1) and Pt/ZT (1:1) catalysts under the NO + CH₄ reaction (in the absence of O₂) were recorded at different temperatures. These spectra are shown in Fig. 4. The Pt/ZT (9:1) catalyst exhibits a moderately intense band at 2037 cm⁻¹ and a less intense one at 2206 cm⁻¹ (Fig. 4). In principle, the band at 2037 cm⁻¹ could be associated with some carbonyl species, but CO is absent in the feed stream. A band at a similar wavenumber has been observed by several authors upon the decomposition of adsorbed CO₂ [13]. However, this is not the case here because we had already detected a weak band upon hydrogen pretreatments, which

vanished at temperatures higher than 623 K. The assignment of this band to NO species can be ruled out because it is absent if a flow of NO (no CH₄ in the feed stream) is passed over the sample; only a weak band at 1800 cm⁻¹, due to a mononitrosyl adsorbed on Pt whose intensity increases with temperature, was discerned. Thus, it can be inferred that the origin of the band must lie in isocyanate (–NCO) or cyano (–CN) species. Isocyanates have been widely documented and discussed as intermediate species in the SCR reaction of NO with hydrocarbons in the presence of O₂, although their frequency falls in the 2300–2160 cm⁻¹ range [18]. Another possibility could be ionic cyano species (–CN), which are thermally stable at high temperatures and are characterised by frequencies in the 2270–2120 cm⁻¹ range [18]. However, the lower frequencies observed in the present work fit in better with that described by Poignant et al. [21] as isocyano (–NC) at 2047 cm⁻¹ on acid Cu-ZSM5 samples. Thus, the band at 2037 cm⁻¹ in Fig. 4 is associated with isocyano –N≡C species. Isocyanate (–NCO) species, which are responsible for the band at 2206 cm⁻¹, appeared to be formed upon oxidation of (–N≡C) species with oxygen pulses [21]. Since in our case no oxygen was fed into the reaction cell, it can be assumed that the isocyano species may be oxidised by the water produced in the NO + CH₄ reaction.

DRIFT spectra for the Pt/Z catalyst (Fig. 4) are virtually the same but much less intense. The only difference is that the band at 2047 cm⁻¹ is accompanied by another small band located at 2096 cm⁻¹. Although further work is needed for a precise assignment, we tentatively ascribe this latter band to cyano-type species. Finally, the absence of any bands in the Pt/ZT (1:1) catalyst, in which the SMSI state is developed, indicates that no stable intermediate species are present on the catalyst surface when this is subjected to the NO + CH₄ reaction.

4. Conclusions

The DRIFT spectra of Pt/ZT catalysts recorded for the in situ NO + CH₄ reaction allow us to draw the following conclusions: (i) Catalyst performance is strongly dependent on the pre-reduction temperature of the catalysts. For the Ti-rich catalysts, platinum particles develop the SMSI state when reduced at

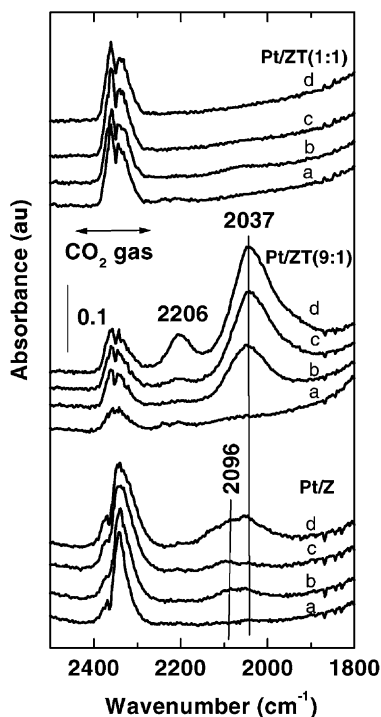


Fig. 4. DRIFT spectra of NO + CH₄ reaction in the 473 K (a), 573 K (b), 673 K (c) and 723 K (d) on Pt/Z, Pt/ZT (9:1) and Pt/ZT (1:1) catalysts.

temperatures higher than 473 K, becoming inactive for the $\text{NO} + \text{CH}_4$ reaction. However, Zr-rich catalysts can be pre-reduced at temperatures as high as 773 K because for such compositions the SMSI state of platinum particles is not developed. Photoelectron spectroscopy precludes coverage effects of the Pt particles by TiO_x fragments when the SMSI state is developed because the Pt signal is not depleted upon pre-reduction at 773 K; (ii) Nitrite/nitrate species are developed on the surface of the Zr-containing catalysts, but are almost absent in the Pt/T catalyst. The presence of these species on the surface, which reaches a maximum for the Pt/ZT (1:1) catalyst, is an indirect measure of catalyst acidity; (iii) The DRIFT spectra of the catalysts subjected to the reaction of NO with CH_4 in the absence of oxygen reveals the formation of isocyano ($-\text{N}\equiv\text{C}$) species. Since the intensity of this band is higher for the Pt/ZT (9:1) catalyst, it is concluded that these species are generated on the Pt–support interface.

Acknowledgements

One of us (RM) is grateful to the Ministry of Science and Technology, Spain, for financial support. This research was partially supported by CONACYT, México.

References

- [1] M. Shelef, *Chem. Rev.* 95 (1995) 209.
- [2] Y. Nishizaka, M. Misono, *Chem. Lett.* (1993) 1296.
- [3] J.N. Armor, *Catal. Today* 26 (1995) 147.
- [4] Y. Li, J.N. Armor, *Appl. Catal. B* 2 (1993) 239.
- [5] E.P. Reddy, T.C. Rojas, A. Fernández, *Langmuir* 16 (2000) 4217.
- [6] C.-M. Lu, Y.-M. Lin, I. Wang, *Appl. Catal. A* 198 (2000) 223.
- [7] Y. Li, J.N. Armor, *J. Catal.* 145 (1994) 393.
- [8] J.O. Petunchi, W.K. Hall, *Appl. Catal. B* 2 (1993) L17.
- [9] J.T. Miller, E. Glusker, R. Peddi, T. Zheng, J.R. Regalbuto, *Catal. Lett.* 51 (1998) 15.
- [10] C.J. Loughran, D.E. Resasco, *Appl. Catal. B* 7 (1995) 113.
- [11] D.A. Shirley, *Phys. Rev.* 35 (1972) 4909.
- [12] R. Pérez, A. Gómez-Cortés, R. Mariscal, J.L.G. Fierro, G. Díaz, to be presented in the 17th Meeting of the North American Catalysis Society, Toronto, Canada, 2001.
- [13] M.C.J. Bradford, M.A. Vannice, *J. Catal.* 173 (1998) 157.
- [14] J.A. Anderson, *J. Chem. Soc., Faraday Trans.* 88 (1992) 1197.
- [15] J.H. Bitter, K. Seshan, J.A. Lercher, *J. Catal.* 171 (1997) 279.
- [16] A. Boix, R. Mariscal, J.L.G. Fierro, *Catal. Lett.* 68 (2000) 169.
- [17] T. Tanaka, T. Okuhara, M. Misono, *Appl. Catal. B* 4 (1994) L1.
- [18] K.I. Hadjiivanov, *Catal. Rev.-Sci. Eng.* 42 (2000) 71.
- [19] E. Kikuchi, K. Yogo, *Catal. Today* 22 (1994) 73.
- [20] Y. Kintaichi, M. Haneda, M. Inaba, H. Hamada, *Catal. Lett.* 48 (1997) 121.
- [21] F. Poignant, J. Saussey, J.-C. Lavalley, G. Mabilon, *Catal. Today* 29 (1996) 93.